SSRG International Journal of Civil Engineering
ISSN: 2348-8352/ https://doi.org/10.14445/23488352/IJCE-V12I6P114

Volume 12 Issue 6, 177-189, June 2025

Original Article

Using AHP-Entropy Method to Evaluate the Effect of Specific Surface Area of Manganese Slag on Concrete Properties: A Case Study on Sustainable Cementitious Materials

Feng Li[1,2], Chee Khoon Ng[1,*], Qiujin Zhao[1]

[1]*Department of Civil Engineering, Faculty of Engineering, Universiti Malaysia Sarawak, Kota Samarahan, Sarawak, Malaysia.*
[2]*Faculty of Civil Engineering, Henan Institute of Engineering, Zhengzhou, Henan, China.*

[*]*Corresponding Author : baiyulan0371@163.com*

Received: 11 April 2025 Revised: 15 May 2025 Accepted: 14 June 2025 Published: 28 June 2025

Abstract *- This investigation examines the viability of employing Manganese Slag (MnS), an industrial by-product, as a sustainable Supplementary Cementitious Material (SCM) in concrete. MnS with four distinct Specific Surface Area (SSA) values (60, 120, 235, and 400 m²/kg) is assessed for its effects on workability, mechanical characteristics, and durability. Concrete specimens were fabricated by substituting different proportions of cement (by mass) with MnS, and their performance was evaluated through slump tests, compressive and flexural strength measurements, freeze-thaw resistance, sulfate attack, and chloride ion penetration analyses. The findings suggest that heightened SSA generally improves fluidity, strength, and durability, with better overall performance observed at 235-400 m²/kg SSA and 5-15% substitution. To find the optimal mixture design, the Analytic Hierarchy Process (AHP) and entropy methodology were utilized, and it was concluded that the most balanced overall performance of concrete was obtained at 235 m²/kg SSA and 10% substitution. This research establishes that MnS when appropriately processed and incorporated, can improve concrete properties while promoting sustainable industrial waste management. These outcomes advance the development of environmentally conscious construction materials and optimize SCM applications in cementitious systems.*

Keywords *- Analytic Hierarchy Process, Entropy method, Manganese Slag, Specific Surface Area, Sustainable.*

1. Introduction

The cement industry confronts significant challenges in global sustainable development because of its high resource consumption, energy demands and carbon emissions. In recent years, diverse artificial and Natural Supplementary Cementitious Materials (SCMs), such as fly ash, slags, silica fume and natural pozzolanic materials, have been extensively used to reduce cement usage, lower environmental impacts and enhance concrete performance [1-3]. Among these, Manganese Slag (MnS), a by-product of granulated blast-furnace slag, demonstrates potential hydraulic and pozzolanic activity, making it a viable alternative for partial cement replacement. However, its low reactivity has restricted its application primarily to low-value uses, such as road filling, backfilling and brick production. This study focuses on MnS as the research object, exploring its potential as one type of SCM aiming to reduce cement consumption and environmental pollution. The key contribution of this study is the systematic revelation of the effect of MnS SSA on the workability, mechanical properties, and durability of concrete. In addition, this study innovatively constructed a multi-criteria decision-making framework, which comprehensively evaluated the multidimensional performance indicators of MnS concrete through the AHP-entropy method, achieving the optimal selection of SSA and providing a scientific basis for the engineering application of MnS in concrete.

From the perspective of industrial structure, China has significant advantages in global Electrolytic Manganese Metal (EMM) production, accounting for 96.5% of the global total in 2020 [4, 5]. The EMM manufacturing process generates vast amounts of Electrolytic Manganese Slag (EMS), which is predominantly disposed of through open-air storage or landfilling [6]. This storage method occupies extensive land resources and results in severe environmental contamination from pollutants leaching into soil and groundwater, such as ammonia nitrogen, sulfates and heavy metals. Although some enterprises have implemented anti-seepage measures, environmental pollution remains a critical concern, posing social, economic and ecological sustainability risks. Therefore, exploring efficient utilization strategies for manganese slag, particularly cementitious materials, is crucial for environmental protection and industrial sustainability. Recent studies have indicated that mechanical activation, particularly through fine grinding, effectively enhances the pozzolanic activity of manganese slag [7, 8]. By increasing its Specific Surface Area (SSA), the hydration-reaction rate and cementitious properties of MnS improve significantly [9, 10]. Research on the impact of SSA variation on the performance of concrete remains insufficient. Existing studies have primarily focused on the effects of MnS replacement ratios on the mechanical properties of concrete, while systematic investigations into how SSA variations influence concrete's workability, strength, and durability are still lacking. In particular, the effect of SSA on concrete slumps has not been thoroughly investigated despite its practical significance in construction. Moreover, the mechanical properties of concrete, mainly compressive and flexural strength, are strongly influenced by the reactivity and filler effect of MnS, both of which are closely linked to its SSA. Although it is generally recognized that higher SSA can enhance strength, the optimal SSA required to balance strength and durability remains unclear. In addition, the durability of MnS-based concrete under aggressive environmental conditions such as chloride ion penetration, freeze-thaw cycles and sulphate attack has received limited attention concerning SSA variation, hindering a full understanding of its long-term performance and sustainability. Furthermore, most existing studies rely on single-variable experimental approaches, lacking multi-criteria decision-making methods for optimal SSA selection [11, 12]. As a result, current applications of MnS in construction materials remain largely low-end, failing to fully utilize its potential as a reactive cementitious component.

To address these gaps, this study systematically investigates the effects of different SSA levels (60, 120, 235, and 400 m²/kg) on the workability, mechanical performance, and durability of MnS-based concrete, using concrete without MnS as the control group. A multi-criteria decision-making framework has been developed based on the Analytic Hierarchy Process (AHP) and Entropy Weight (AHP-EW) method to optimize SSA selection. Integrating subjective expert judgment with objective data-driven weighting ensures a comprehensive evaluation of SSA configurations. It systematically evaluates experimental data using traditional single-weight and comprehensive-weight methods (Ideal AHP-entropy Method). The main contributions of the research are reflected in three aspects. Firstly, a systematic evaluation framework covering the workability, mechanical properties, and durability of concrete was constructed, comprehensively examining the effect of MnS SSA on its performance. Secondly, the innovative introduction of an optimization model based on the AHP-entropy method significantly enhances the scientific and objective nature of the SSA selection process. Finally, practical data was provided for the sustainable utilization of MnS.

The structure of this article is as follows: Section 2 systematically reviews relevant literature, focusing on the cement-based properties of MnS, the effect of SSA on concrete properties, and the application of AHP and entropy weight method in material optimization. Section 3 elaborates on the research methodology system, including experimental design, testing process, and the construction process of the AHP entropy weight model. Section 4 provides an in-depth analysis of the experimental results and explores decision optimization strategies based on the model. Section 5 summarizes the core research findings, explains the engineering application value, and looks forward to future research directions.

2. Literature Review

2.1. Utilization of MnS as a Supplementary Cementitious Material

The global construction industry increasingly emphasises using industrial by-products as SCMs to reduce cement consumption, improve concrete properties, and mitigate environmental impact. Among these industrial by-products, MnS, as a typical by-product in the production process of EMM, has shown broad prospects as a substitute for traditional cement materials due to its potential hydraulic and volcanic ash activity [13]. Compared with other industrial by-products such as Ground Granulated Blast Furnace Slag (GGBFS) and fly ash, although MnS has similar performance characteristics, its practical application in concrete engineering is still limited due to its inherent low reactivity and poor chemical composition stability [14]. Previous studies have shown that MnS can be successfully integrated into cement-based systems as an effective binder or filler material in cement-based composite materials. Its chemical composition includes key components such as silicon dioxide (SiO_2), alumina (Al_2O_3), calcium oxide (CaO), and manganese oxides (MnO), which have a significant impact on the potential properties of its reactive materials [15, 16]. Due to MnS's low initial reactivity, mechanical (e.g., ultrafine grinding) and chemical (e.g., alkali treatment) activation methods are crucial for enhancing its cement performance [17]. Despite technological advances, the optimal processing of MnS, particularly its SSA effects on concrete, remains understudied.

2.2. Effect of SSA on the Reactivity of MnS

Mechanical activation (mainly via fine grinding) is the most effective method to enhance industrial slag reactivity

[18]. As the key parameter for measuring material reactivity, SSA directly reflects the available reaction surface area per unit mass and is critical in determining MnS's volcanic ash activity. Research demonstrates that moderate increases in SSA for traditional SCMs like GGBFS enhance hydration kinetics, particle packing, and secondary reactions, thereby improving concrete performance [19, 20]. It is worth noting that the hydration activity index of GGBFS shows an approximately linear positive correlation with SSA. However, when SSA exceeds 350 m^2/kg, this gain trend will gradually flatten out due to the enhanced particle aggregation effect [21]. Studies confirm that MnS's SSA determines its reactivity with calcium hydroxide ($Ca(OH)_2$) to form Calcium Silicate Hydrate (CSH) gels, which improve concrete properties [22]. However, excessive grinding (>400 m^2/kg) may lead to negative effects, including decreased hydration efficiency, elevated water demand, and intensified particle agglomeration [23]. Thus, determining MnS's optimal SSA range remains a critical research need, impacting both material performance and sustainable construction applications.

2.3. Impact of MnS on Workability and Mechanical Properties of Concrete

The workability of concrete is a key factor affecting construction efficiency and overall performance of concrete. Research has shown that MnS can alter the fresh state of concrete by affecting water usage and slurry viscosity. When MnS replaces 20% cement, it significantly improves the workability of concrete, resulting in a 157% increase in slump. However, when the substitution ratio exceeds 30%, the working performance decreases due to the increased water consumption caused by the high SSA of small MnS particles [24]. Similar trends have also been observed in the GGBFS and fly ash study, where the optimal balance between fineness and substitution ratio is crucial for maintaining workability [25].

The effect of MnS on the mechanical properties of concrete has been widely studied. Research has shown that a MnS substitution rate of 10–30% can enhance compressive strength by improving the density and microstructure of the cementitious matrix [26]. However, excessive MnS content (>40%) can lead to a decrease in strength due to dilution of clinker content and a reduction in early hydration rate [27]. The synergistic effect of MnS with other admixtures, such as fly ash, can enhance mechanical properties by improving particle arrangement and hydration efficiency [28]. The SSA of SCMs has long been recognized as a key factor influencing their reactivity and performance in concrete. Previous studies have demonstrated that higher SSA enhances pozzolanic activity by increasing the available surface for reaction and promoting microstructural densification [29]. This is particularly evident in materials such as silica fume and ultrafine fly ash, where improved fineness correlates with better mechanical properties and durability.

2.4. Durability Performance of MnS Concrete

Durability remains a critical consideration for MnS concrete, particularly within aggressive environmental conditions involving freeze-thaw cycles, chloride-ion penetration, and sulfate attack. Several studies have explored the resistance of MnS concrete towards these durability factors. Incorporating 20% MnS reduced strength loss by 15% after 50 freeze-thaw cycles, although excessive MnS (>30%) may negatively affect volume stability [30]. Twenty per cent MnS replacement reduced chloride-ion penetration by 25%, while 30% MnS replacement led to a 40% decrease in chloride migration [27, 31]. However, the impact of SSA on chloride resistance remains unclear. For sulfate attack, 20% MnS reduced mass loss and strength degradation by 22% and 30%, respectively, owing to stable hydration product formation [32]. Research on fly ash with varying fineness levels has demonstrated that moderate increases in SSA improve compressive strength and sulfate resistance. In contrast, excessive fineness may lead to higher water demand and reduced workability [33]. Other studies have indicated that ultrafine mineral admixtures can enhance densification and impermeability. However, they may also cause particle agglomeration at high dosages, negatively impacting long-term durability and increasing the risk of shrinkage [34]. At MnS levels exceeding 35%, sulfate resistance declined because of insufficient primary hydration compounds. Despite these findings, further research is needed to identify the optimal SSA of MnS for enhancing durability in concrete applications.

2.5. Application of AHP-Entropy Method in Concrete Optimization

Multi-Criteria Decision-Making (MCDM) approaches have been widely employed in evaluating and optimizing material properties in construction. The Analytic Hierarchy Process and AHP-EW rank among the most effective techniques for comprehensive evaluation, as they integrate subjective expert judgments with objective statistical analyses [35]. The Analytic Hierarchy Process has been applied in various fields, including construction material selection, environmental sustainability assessments, and structural health monitoring [36]. The entropy method quantifies each criterion's contribution based on data variability, making it ideal for optimizing performance indicators such as strength, durability, and workability [37].

In practical application, a single method may make it challenging to reflect each indicator's contribution fully. Many studies have used a combination of weighting or mixed evaluation methods, such as the AHP-entropy method [38, 39]. Several studies have successfully implemented the AHP-EW framework in material optimization. This method has optimized cleanroom ventilation systems [40] and enhanced railway track evaluations [41]. Combining AHP with entropy weighting in concrete materials has improved decision-making accuracy in assessing concrete durability [42].

However, research concerning AHP-EW applications in optimizing the SSA of MnS for concrete remains insufficient.

Despite substantial advancements in MnS research, several critical gaps persist. Further research is needed to investigate the effects of MnS SSA on the workability (especially slump and mortar flowability) and mechanical properties of concrete. There is still limited research on MnS SSA's effects on concrete's durability, including freeze-thaw resistance, chloride ion penetration, and sulfate corrosion. In addition, the combination of AHP and entropy method has not yet been applied to optimize MnS SSA, highlighting the necessity of establishing a comprehensive decision-making model to determine the optimization of SSA to improve the comprehensive performance of concrete.

This study aims to analyze the effects of MnS SSA on the workability, mechanical properties, and durability of concrete through experiments and to apply the AHP-entropy method to analyze the optimized configuration of SSA that affects the comprehensive performance of concrete. This provides a scientific basis for the engineering application of MnS in concrete and fills the research gap.

3. Materials and Methods

3.1. Experimental Design

The property evaluation of MnS concrete is based on a series of standardized experimental methods. Among them, the workability of freshly mixed concrete is determined through standard slump tests, which strictly follow established operating procedures [43]. The mechanical properties of concrete are evaluated through compressive strength and flexural strength tests. Compressive strength was measured on 150-mm × 150-mm × 150-mm cubic specimens after 3, 7, and 28 days of curing using a YAW-4306 automatic pressure testing machine (Figure 1). Flexural strength was determined using the three-point bending method on prism specimens (150 mm × 150 mm × 750 mm), with the load applied at the midpoint of the span [44, 45]. Durability was assessed through chloride-ion penetration, sulfate attack, and freeze-thaw resistance tests [46-49].

The rapid electric flux method was employed on cylindrical specimens (Φ100 mm × 50 mm) after 28 and 56 days of curing to determine chloride permeability. Sulfate resistance was evaluated by immersing specimens in a 5% Na_2SO_4 solution for up to 180 days, with mass loss and compressive-strength degradation recorded periodically. Freeze-thaw resistance was tested over 300 cycles between -17°C and 5°C, tracking mass loss and compressive strength at 25-cycle intervals. Finally, microscopic analysis using Scanning Electron Microscopy (SEM) was conducted to investigate the hydration products and internal microstructure of MnS concrete, providing insights into the material's macro-level performance characteristics.

Fig. 1 Concrete mechanical tests

3.2. Material and Data

To investigate the effect of the SSA of MnS on concrete properties, MnS was selected as the primary supplementary cementitious material. The material came from a metal-smelting plant in Xingyang City, Henan Province. Because the slag had been stored outdoors for an extended period, it contained impurities and appeared grey-black and block-like.

Manganese slag was chosen based on several key criteria: its abundance and low cost as an industrial by-product, its high reactivity after grinding, its pozzolanic potential, making it suitable for partial cement replacement, and its significant environmental benefits through resource recycling and waste reduction.

The MnS was analyzed to determine its fundamental physical properties. Its moisture content was measured using the drying method at 105 ± 5°C, yielding an average natural moisture content of 21.1%. This high moisture level demonstrated the need for drying the material to minimize environmental contamination.

The density of the dried MnS, determined by the pycnometer method, was 2.911 g/cm³. MnS was mechanically activated by grinding, and the samples appear in Figure 2. MnS was ground into four groups with SSA of 60, 120, 235, and 400 m²/kg. Concrete without MnS was used as the control group for comparison.

In conjunction with MnS, several essential materials were selected and characterized to ensure a reliable mix design. The study used 42.5-grade ordinary Portland cement produced in Henan, China. The fine aggregate consisted of Grade II medium sand with a fineness modulus 2.69. The coarse aggregate comprised gravel ranging from 5 to 20 mm in particle size, exhibiting an apparent density of 2,645 kg/m³ and a silt content of 0.3%. The key physical and mechanical properties of the cement and aggregates were tested to confirm their suitability for the experimental program, as summarized in Table 2 and 3.

Fig. 2 Manganese slag samples

Table 1. Physical and mechanical properties of cement and sand

Property	Cement	Sand
Density	3.04 g/cm³	2675 kg/m³
Specific Surface Area (SSA)	348 m²/kg	—
28-day Compressive Strength	54.9 MPa	—
28-day Flexural Strength	9.1 MPa	—
Mud Content	—	2.4%

To ensure consistency and property of the mixtures, clean, potable water served as the mixing water throughout the study. Additionally, a polycarboxylic acid-based water-reducing admixture from Henan, China, was used to improve the workability and dispersion of the cementitious materials.

Table 2. Performance indexes of water-reducing agent

Property	Value
Solid Content (%)	24.92
PH	8.25
Density (kg/m³)	1.12
Water Reduction Rate (%)	27

3.3. AHP-Entropy Method for Comprehensive Evaluation

Given the complexity of evaluating multiple performance indicators, a hybrid AHP-Entropy method was applied to assign subjective and objective weights to each indicator. The Analytical Hierarchy Process (AHP) was used to model the evaluation structure, construct the pairwise judgment matrix, and derive subjective weights through eigenvector computation and consistency checking. Meanwhile, the entropy method objectively calculated weights based on the information entropy derived from the standardized raw data matrix. The combination of these two methods yielded comprehensive weights, ensuring a balanced and robust assessment of the impact of MnS-SSA on concrete performance. The detailed calculation process of the AHP-Entropy method is illustrated in Figure 3.

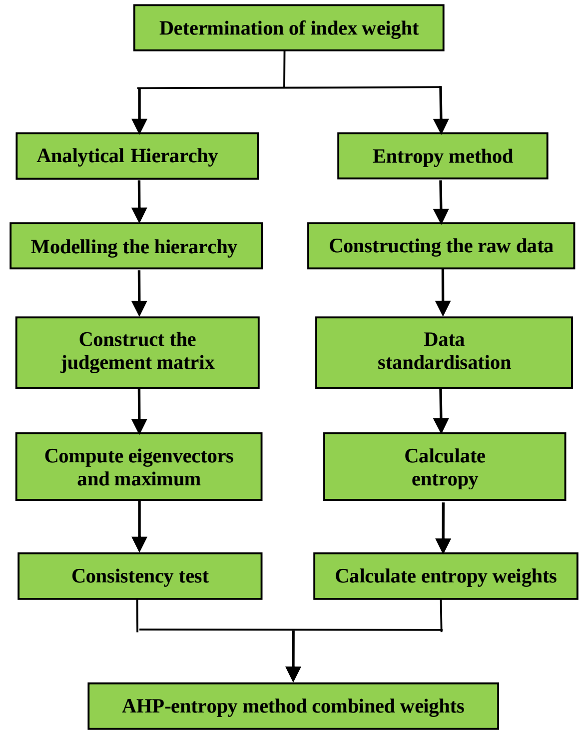

Fig. 3 Flow chart of AHP-entropy method of comprehensive weight calculation

Table 3. A hierarchical analysis structure model for comprehensive performance analysis of MnS concrete

overall objectives	criteri	sub-criteria
Specific surface area optimization analysis of MnS concrete (A)	Workability and mechanical	Slump (C1)
		Compressive strength (C2)
		Flexural strength(C3)
	Durability (B2)	Electric flux in chloride ion corrosion (C4)
		Mass loss in sulfate corrosion (C5)
		Compressive strength corrosion resistance coefficient (C6)
		Mass loss rate under F-T cycles (C7)
		Compressive strength loss under F-T cycles (C8)

A hierarchical model was constructed to effectively apply the calculated weights to the evaluation framework based on the specific surface-area optimization objective of MnS concrete. This model organizes the performance indicators across multiple levels, ranging from overall objectives to evaluation criteria and sub-criteria, thereby providing a structured foundation for comprehensive analysis using the combined AHP-Entropy weight method.

3.3.1. AHP Method

A hierarchical analysis model was constructed to evaluate the comprehensive performance of MnS concrete. The model comprises four levels: the overall goal (Level 0), two criteria levels (Levels 1 and 2), and the alternatives layer (Level 3). Judgment matrices were established between adjacent levels to quantify the relative importance of elements. Specifically, matrix A1 reflects the comparisons between the primary criteria, B1 and B2 (Level 0 to Level 1). In contrast, matrices B1 and B2 represent the comparisons among sub-criteria under each criterion - C1, C2, and C3 under B1, and C4 through C8 under B2 (Level 1 to Level 2). These matrices are expressed, respectively, as:

$$A1= [B1, B2] = \begin{bmatrix} 1 & 1/A12 \\ A12 & 1 \end{bmatrix} \tag{1}$$

$$B1= [C1, C2, C3] = \begin{bmatrix} 1 & 1/B12 & 1/B13 \\ B12 & 1 & 1/B23 \\ B13 & B23 & 1 \end{bmatrix} \tag{2}$$

$$B2= [C4,C5,C6,C7,C8] = \begin{bmatrix} 1 & 1/C12 & 1/C13 & 1/C14 & 1/C15 \\ C12 & 1 & 1/C23 & 1/C24 & 1/C25 \\ C13 & C23 & 1 & 1/C34 & 1/C35 \\ C14 & C24 & C34 & 1 & 1/C45 \\ C15 & C25 & C35 & C45 & 1 \end{bmatrix} \tag{3}$$

Based on these hierarchical structures, a judgment matrix was constructed using Saaty's nine-point scale to compare the relative importance of performance indicators. A consistency check was performed using the Consistency Index (CI) and Consistency Ratio (CR) to ensure logical coherence in expert evaluations.

Applying Saat’s nine-point scale enables a systematic, quantitative expression of expert judgments in the pairwise-comparison process. Specifically, a value of 1 indicates equal importance between two factors, while values of 3, 5, 7, and 9 correspond to increasing levels of importance—moderate, strong, very strong, and absolute importance of one factor over another. Intermediate values, such as 2, 4, 6, and 8, can be used to express compromise between adjacent judgments. For instance, if factor i is judged to be strongly more important than factor j, it would receive a value of 5. Conversely, the reciprocal value (e.g., 1/5) is used when j is compared with i, ensuring the construction of a positive reciprocal matrix.

Based on the completed judgment matrices, the subjective weights of indicators were derived using the normalized principal eigenvector method, which reflects the relative importance of each factor as perceived by experts. When comparing the importance of performance factors in manganese slag concrete, it is essential to conduct consistency testing on all judgment matrices to ensure logical coherence and reliability. This process enhances the scientific rigour and credibility of the decision-making results. In the AHP, commonly used consistency-testing metrics include the Consistency Index (CI) and the Consistency Ratio (CR). The calculation methods for these two metrics are provided in Equations 4 and 5.

$$CI = \frac{\lambda_{max} - n}{n - 1} \tag{4}$$

$$CR = \frac{CI}{RI} \tag{5}$$

Among them, λ_{max} = the largest eigenvalue of the judgment matrix, n denotes the order of the matrix, and RI = the average random consistency index for the matrix, with values provided in 3.3.2. Entropy *Method*

The entropy method was employed to determine objective indicator weights based on the degree of data dispersion. Raw experimental data were standardized using the extremum method, with equations applied individually for:

Positive indicators (e.g., compressive strength)

Table . If CI = 0, it demonstrates that the matrix possesses perfect consistency. When CI approximates 0, it suggests that the matrix exhibits a high degree of consistency. If CR is less than 0.1, the judgment matrix is considered to have acceptable consistency; otherwise, the judgment matrix requires adjustment. As shown in Table 4, the RI value increases progressively with matrix order *n*, indicating that the likelihood of random inconsistency rises as the number of criteria expands. This trend underscores the importance of the Consistency Ratio (CR = CI / RI), which adjusts the raw Consistency Index (CI) relative to the matrix size, ensuring a fair assessment. Therefore, accurate reference to RI values is critical when determining whether a pairwise comparison matrix meets the acceptable threshold of logical consistency.

3.3.2. Entropy Method

The entropy method was employed to determine objective indicator weights based on the degree of data dispersion. Raw experimental data were standardized using the extremum method, with equations applied individually for:

Positive indicators (e.g., compressive strength)

Table 4. Values of average random consistency index RI [50]

Matrix order n	1	2	3	4	5	6	7	8	9
RI	0	0	0.58	0.90	1.12	1.24	1.32	1.41	1.45

$$y_{ij} = \frac{x_{ij} - \min(x_{ij})}{\max(x_{ij}) - \min(x_{ij})} \quad (6)$$

Negative indicators (e.g., mass loss rate)

$$y_{ij} = \frac{\max(x_{ij}) - x_{ij}}{\max(x_{ij}) - \min(x_{ij})} \quad (7)$$

Moderate indicators (e.g., slump)

$$y_{ij} = \frac{\left| x_{ij} - \frac{\max(x_{ij}) + \min(x_{ij})}{2} \right|}{\max(x_{ij}) - \min(x_{ij})} \quad (8)$$

The information entropy of each indicator was computed to determine data variability. Objective weights were then determined using entropy differentiation coefficients.

$$p_{\mathrm{ij}} = \frac{y_{\mathrm{ij}}}{\sum_{i=1}^{m} y_{\mathrm{ij}}} \quad (9)$$

$$e_{\mathrm{j}} = -\ln n \sum_{i=1}^{m} p_{\mathrm{ij}} \ln p_{\mathrm{ij}} \quad (10)$$

In this context, p_{ij} represents the proportion or contribution of the MnS concrete SSA modification scheme, while e_j denotes the entropy value of the indicator. The objective weight coefficients of the performance indicators can be determined using equations (12).

$$g_{\mathrm{j}} = 1 - e_{\mathrm{j}} \quad (11)$$

$$S_{\mathrm{j}} = \frac{g_{\mathrm{j}}}{\sum_{j=1}^{n} g_{\mathrm{j}}} \quad (12)$$

Among them, g_{j} represents the differentiation coefficient of the indicator, while S_{j} denotes the indicator's objective weight coefficient.

3.3.3. Calculation of Combined Weights and Performance Evaluation

The final composite weights (Z_j) of performance indicators were obtained using a 50:50 combination of AHP-derived subjective weights (W_j) and Entropy-derived objective weights (S_j):

$$Z_{\mathrm{j}} = 0.5 \times W_{\mathrm{j}} + 0.5 \times S_{\mathrm{j}} \quad (13)$$

Where Z_j represents the comprehensive weight, and W_j and S_j denote the subjective and objective weights of the indicator, respectively.

The comprehensive performance score for each SSA-modified concrete mix was then calculated as follows:

$$f(c) = \sum_{i=1}^{8} \left(Z_j y_i \right) \quad (14)$$

Where y_i represents standardized test data, while Z_j represents the combined weight of each performance indicator.

4. Results

4.1. Experimental Results

This study comprehensively investigated the effects of MnS, with varying SSA, on the workability, mechanical properties, and durability of concrete. Results showed that, compared to the control group (the concrete without MnS addition), increasing SSA generally improved the slump of concrete at lower replacement levels (≤10%wt), especially at SSA = 235 m²/kg with 5%wt, where optimal flowability and particle packing were achieved. However, excessive replacement (≥15%wt) led to a sharp decline in workability due to increased water demand and particle agglomeration. Regarding mechanical performance, compressive and flexural strengths were significantly enhanced at moderate SSA (235–400 m²/kg) with 10–15%wt MnS replacement. For compressive strength at a curing age of 28 days, combinations of SSA = 235 m²/kg with 15%wt and SSA = 400 m²/kg with 10%wt achieved the maximum compressive strength (57 MPa), which was 1.79% higher than that of concrete without MnS. Meanwhile, regarding flexural strength, these combinations at 28 days exhibited a flexural strength (6.1 MPa) that was 2.87% higher than that of concrete without MnS. Conversely, lower SSA or higher replacement levels (>15%wt) reduced strength due to limited pozzolanic activity and excessive dilution of cementitious materials.

The Specific Surface Area (SSA) positively correlated with workability, compressive strength, and flexural strength at moderate levels (SSA = 235–400 m²/kg, 10–15%wt). However, excessive SSA reduced performance at higher dosages (⩾15%wt) due to agglomeration and water demand. Overall, SSA enhances concrete properties up to an optimal point, beyond which performance declines, indicating a nonlinear, dosage-dependent relationship.

Scanning electron microscopy analysis further confirmed that higher SSA improved microstructure densification through enhanced hydration and a continuous CSH gel network formation. When MnS replaces 10 wt% of cement, the SSA of MnS has differentiated impacts on five concrete durability indicators. For chloride ion penetration resistance at 56 days, SSAs of 235 m²/kg and 400 m²/kg decrease the electric flux (Q) by approximately 56.15% compared to 0 wt%, enhancing chloride resistance. Regarding sulfate corrosion resistance, after 180 days in a sulfate environment, an SSA of 400 m²/kg reduces the mass loss rate (W_L) by 79.5% and increases the compressive strength corrosion resistance coefficient (K_f) by 3.2% compared to 0 wt%, improving concrete resistance to sulfate corrosion. In terms of freeze-thaw cycle resistance, after 200 cycles, SSAs of 400 m²/kg and 120 m²/kg increase the mass loss rate in the freeze-thaw cycle (Md) by 39.2% and 49.0%, respectively, compared to 0 wt%, and an SSA of 400 m²/kg shows a 62.4% increase in compressive strength loss rate (f_t) after 200 cycles. MnS addition reduces frost resistance, with smaller SSA leading to greater mass and strength losses. The experimental results reveal clear correlations between SSA and concrete durability. Chloride resistance improves significantly with higher SSA. At 235 and 400 m²/kg, electric flux decreased by 56%, indicating a strong negative correlation between SSA and permeability. Sulfate resistance also shows a positive correlation with SSA. At 400 m²/kg, mass loss decreased by 79.5%, and strength retention increased by 3.2%, suggesting improved chemical durability. Freeze-thaw resistance exhibits a negative correlation with SSA. Higher SSA (e.g., 400 m²/kg) increases mass and strength losses, indicating reduced frost durability. Overall, SSA enhances chemical durability but may compromise freeze-thaw performance, highlighting the need for balance in SSA selection. The SSA of MnS and cement replacement rate differently affect seven individual performance indicators of concrete's workability, mechanical properties, and durability. Therefore, it is crucial to assess their impact on comprehensive performance and find the optimal combination of SSA and cement replacement rate, which can be addressed by the AHP-entropy method.

4.2. Results Based on the AHP Method

The AHP was applied to evaluate subjectively the influence of eight performance indicators on the comprehensive properties of MnS concrete. Expert judgments determined the weights across workability and mechanical properties (B1) and durability (B2). The results of Table 5 revealed that B1 was significantly more influential (weight = 0.7621) than B2 (weight = 0.2379). Among all secondary indicators, compressive strength (C2) possessed the highest weight (0.4001), followed by slump (C1) at 0.2301 and flexural strength (C3) at 0.1319. For durability indicators, compressive-strength loss under freeze-thaw cycles (C8) ranked highest (0.0836), demonstrating its key role in long-term performance.

These findings indicate that workability and mechanical properties shape overall MnS concrete performance. Notably, the relatively lower weights of durability-related indicators (e.g., C4–C7) suggest that their impact is comparatively limited within the AHP-based evaluation framework. This hierarchical prioritization provides valuable insights for optimizing mixed design strategies, especially when balancing short-term workability and strength with long-term durability requirements.

Table 5. AHP weights

Tier 1 indicators	Weights	Tier 2 indicators	Weights	Comprehensive weight	Ranking
B1	0.7621	C1	0.3019	0.2301	2
		C2	0.5250	0.4001	1
		C3	0.1731	0.1319	3
B2	0.2379	C4	0.0690	0.0164	8
		C5	0.1580	0.0376	6
		C6	0.2826	0.0672	5
		C7	0.1388	0.0330	7
		C8	0.3516	0.0836	4

Note: B1 represents Working and Mechanical Properties, focusing on strength and workability, while B2 represents Durability Properties, assessing long-term resistance to environmental factors. C1 corresponds to slump, indicating workability, and C2–C3 represent Compressive and Flexural Strength, measuring mechanical properties. C4 represents electric flux in chloride ion corrosion. C5–C6 represent mass loss and compressive strength corrosion resistance coefficient in sulfate corrosion, while C7–C8 represent mass loss and compressive strength loss under F-T cycles.

4.3. Results Based on the Entropy Method

The entropy method has objectively evaluated eight indicators based on experimental data from 30 SSA-based concrete configurations. The calculated weights in Table 3 reflect each indicator's variability and informational Content. The most influential indicators were the electric flux under chloride ion corrosion (C4), which had the highest weight of 0.2303, followed by slump (C1) at 0.1942 and flexural strength (C3) at 0.1508. The compressive strength (C2) demonstrated a moderate objective weight of 0.1187, while the sulfate and freeze-thaw resistance indicators showed lower, yet still notable, importance. The results suggest that durability indicators, especially chloride ion penetration resistance (C4), play a critical role in evaluating the comprehensive performance of SSA-based concrete.

Table 3. Entropy weights

Secondary indicator	Entropy value e_j	Differentiation coefficient g_j	Objective weight coefficient S_j
C1	0.9055	0.0945	0.1924
C2	0.9422	0.0578	0.1187
C3	0.9266	0.0734	0.1508
C4	0.8879	0.1121	0.2303
C5	0.9658	0.0342	0.0702
C6	0.9585	0.0415	0.0852
C7	0.9697	0.0303	0.0623
C8	0.957	0.043	0.0883

In contrast, indicators such as sulfate corrosion resistance (C5) and freeze-thaw resistance (C7), essential for long-term durability, exhibited relatively low entropy and differentiation coefficients, leading to lower weights. This implies that these indicators were more stable across the evaluated configurations, offering less contribution to differentiation. Nevertheless, their inclusion remains vital to ensure a holistic assessment of concrete performance under diverse environmental stressors.

4.4. Results Based on the Combined AHP-Entropy Method

The AHP-entropy methods were integrated through an equal-weight linear combination to ensure a balanced evaluation incorporating expert judgment and experimental data. The combined weighting results in Figure 4 identified compressive strength (C2) as the most influential factor (0.2594), followed by a slump (C1) at 0.2122 and flexural strength (C3) at 0.1414. Among durability indicators, electrical flux under chloride ion corrosion (C4) had the highest weight (0.1234). These findings highlight the predominant role of mechanical properties, particularly compressive strength, in performance assessment while emphasizing the significance of durability factors, such as chloride ion resistance, in evaluating manganese slag concrete.

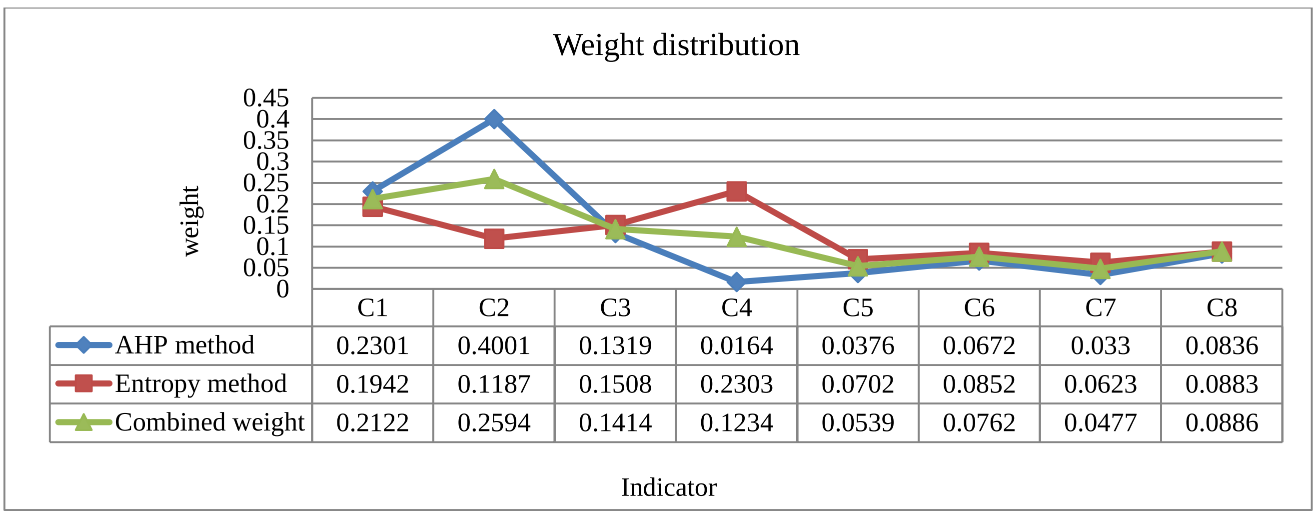

Fig. 4 Combined weight

4.5. Evaluation of Experimental Programs

Based on four Specific Surface Area (SSA) values of MnS (60 m²/kg, 120 m²/kg, 235 m²/kg and 400 m²/kg), a fixed cement-replacement rate of 10%, a curing age of 28 days and six-time parameters (50, 100, 150, 200, 250 and 300), a total of 30 MnS concrete configurations were designed. These configurations underwent comprehensive evaluation using combined weights derived from the AHP-Entropy method. The resulting performance scores, when ranked, identified the optimal mix design, as illustrated in Figure 5. The experimental results presented in Figure 5 illustrate the performance scoring of various MnS concrete formulations under diverse conditions. The highest-scoring mix (Dosage = 0.1, Days = 28, SSA = 235 m²/kg, Time = 50) achieved a score of 0.82, demonstrating superior mechanical properties and durability. Generally, mixtures with higher SSA (235 m²/kg) and shorter curing times (50-150 hours) performed better, presumably due to enhanced reactivity and optimized particle packing. Conversely, formulations with lower SSA (60 m²/kg) and extended curing times (200-300 hours) exhibited markedly lower scores, with the weakest mix scoring 0.17, indicating that insufficient SSA reduces pozzolanic activity and leads to excessive water demand and diminished strength. These results emphasize optimizing

SSA and curing conditions to balance concrete's workability, mechanical properties, and durability. When the SSA of MnS is 235 m²/kg and the curing time is 28 days, its application effect in concrete is most balanced.

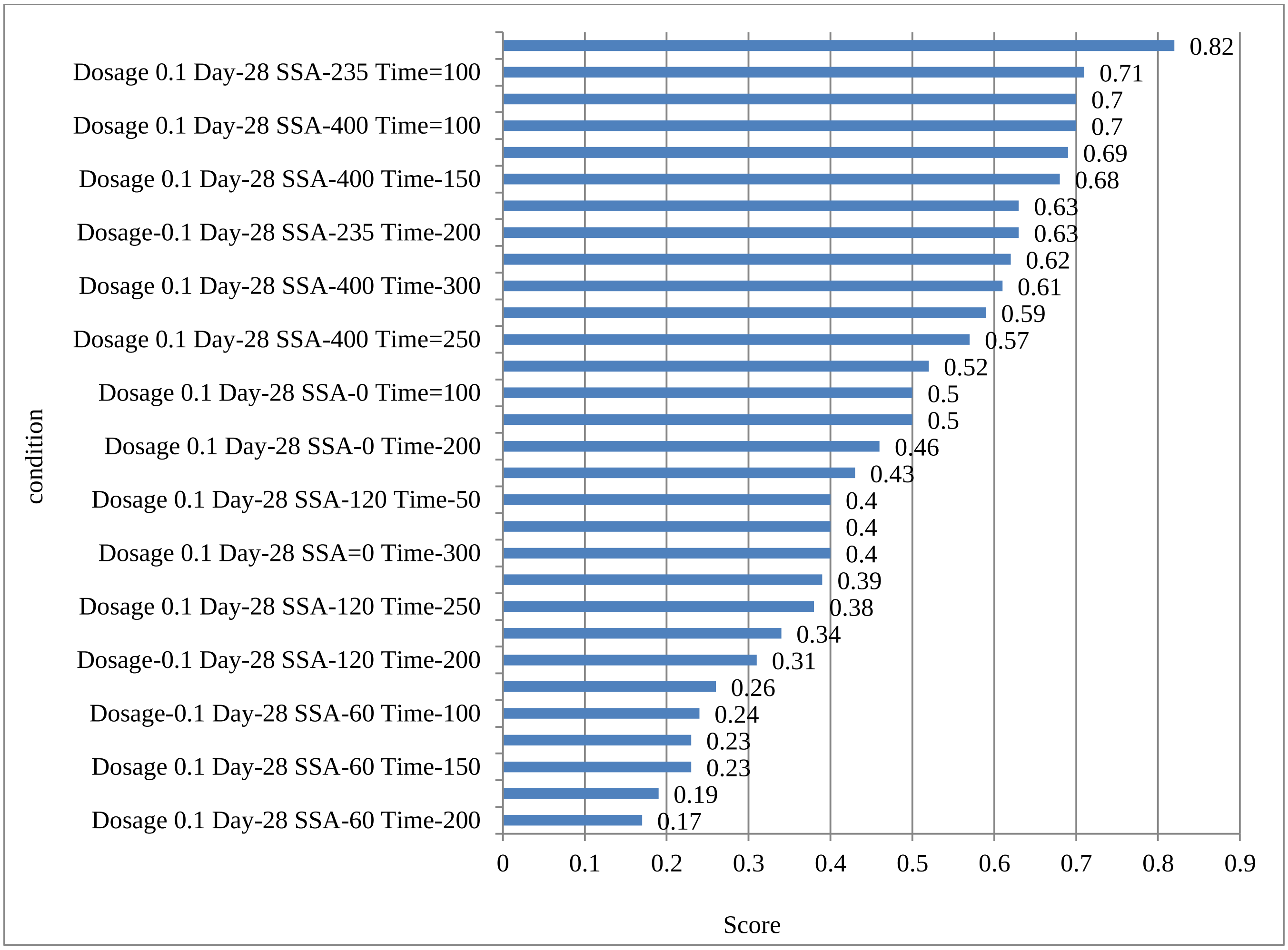

Fig. 4 Scoring of the experimental results

4.6. Comparison with Previous Studies

This study comprehensively explores the influence of MnS SSA on the comprehensive property of concrete, aiming to optimize its application as a substitute for cement. The workability, mechanical properties, and durability of concrete without MnS were systematically evaluated by introducing different SSA (60, 120, 235, and 400 m²/kg) and different cement substitution rates (0–40%wt) compared to the control group without MnS. A key contribution of this work is using the AHP-Entropy method, which provided a structured and quantitative framework to identify the optimal SSA-replacement combination. The findings revealed that increasing SSA generally improved reactivity and performance, especially at moderate levels. Specifically, 235 m²/kg SSA with 10% replacement was identified as the optimal combination, achieving excellent slump, higher compressive and flexural strength, and improved durability against chloride-ion penetration, sulfate attack, and freeze-thaw cycles. These results are consistent with previous studies on SCMs such as fly ash, silica fume, and slag, where higher SSA has been associated with enhanced pozzolanic activity and microstructural densification [29, 33]. However, consistent with earlier findings, excessively high SSA (e.g., 400 m²/kg) increased water demand and reduced long-term performance under certain conditions due to particle agglomeration—confirming trends observed with ultrafine mineral admixtures [34]. Compared to existing literature, this study adds value by providing a systematic SSA-performance mapping for MnS, a relatively underexplored industrial by-product. Moreover, integrating AHP-Entropy analysis offers a novel decision-making tool beyond traditional single-parameter optimization methods. Overall, the study supports earlier research on the importance of SSA in SCMs and offers specific, actionable recommendations for using MnS effectively in sustainable concrete design.

5. Conclusion

This study comprehensively investigated the effects of SSA of MnS on concrete properties, focusing on optimizing its application as a sustainable supplementary cementitious material. By incorporating multiple SSA levels (60, 120, 235, and 400 m²/kg) and various cement replacement ratios (0–40% by weight), this study evaluated key performance metrics—including workability, mechanical properties, and durability—compared to a control group consisting of concrete without MnS. A key innovation was integrating the AHP-Entropy method to analyze and determine the optimal SSA and replacement level systematically.

The findings revealed that increasing SSA enhances both the reactivity and performance of MnS concrete. Specifically, an SSA of 235 m²/kg with a 10%wt replacement ratio was identified as the optimal mix. Concrete demonstrated excellent slump and fluidity at this combination and improved compressive and flexural strength. Through durability assessment, it was found that within the range of SSA = 235–400 m²/kg, the frost resistance, resistance to chloride ion penetration, and resistance to sulfate attack of concrete were enhanced. The AHP entropy method makes the multi-criteria decision-making process more rational, combining subjective evaluations from experts with objective data weights based on entropy. It evaluated that the optimal balance between all performance indicators can be achieved when SSA is 235 m²/kg and the substitution rate is 10%wt, further confirming the applicability of MnS as a cement substitute. The optimized MnS concrete promotes waste resource utilization and reduces cement consumption, demonstrating potential applications in sustainable construction.

This study provides valuable insights into MnS as a sustainable cement-based material, but several limitations exist. The research mainly relies on laboratory-scale experiments and lacks practical application verification through on-site testing. Although higher SSA can enhance reactivity, potential environmental issues such as heavy metal leaching have not been thoroughly explored. In addition, excessive SSA levels (>235 m²/kg) can increase water demand and reduce water availability, and further research is needed.

Future research should optimise SSA while maintaining its performance and explore solutions such as water-reducing agents and modified mechanical grinding processes. Leaching tests are crucial for evaluating environmental impacts, especially pollutant releases. Enhancing the freeze-thaw durability through chemical modification and air-entraining agents is crucial. Finally, large-scale on-site testing is crucial for verifying the long-term performance of MnS concrete and ensuring its practical application as a sustainable building material.

References

[1] V.G. Papadakis, S. Antiohos, and S. Tsimas, "Supplementary Cementing Materials in Concrete: Part II: A Fundamental Estimation of the Efficiency Factor," *Cement and Concrete Research*, vol. 32, no. 10, pp. 1533-1538, 2002. [CrossRef] [Google Scholar] [Publisher Link]

[2] V.G. Papadakis, and S. Tsimas, "Supplementary Cementing Materials in Concrete: Part I: Efficiency and Design," *Cement and Concrete Research*, vol. 32, no. 10, pp. 1525-1532, 2002. [CrossRef] [Google Scholar] [Publisher Link]

[3] Daman K. Panesar, and Runxiao Zhang, "Performance Comparison of Cement Replacing Materials in Concrete: Limestone Fillers and Supplementary Cementing Materials – A Review," *Construction and Building Materials*, vol. 251, 2020. [CrossRef] [Google Scholar] [Publisher Link]

[4] Dengquan Wang, Qiang Wang, and Junfeng Xue, "Reuse of Hazardous Electrolytic Manganese Residue: Detailed Leaching Characterization and Novel Application as a Cementitious Material," *Resources, Conservation and Recycling*, vol. 154, 2020. [CrossRef] [Google Scholar] [Publisher Link]

[5] Jirong Lan et al., "Selective Recovery of Manganese from Electrolytic Manganese Residue by Using Water as Extractant under Mechanochemical Ball Grinding: Mechanism and Kinetics," *Journal of Hazardous Materials*, vol. 415, 2021. [CrossRef] [Google Scholar] [Publisher Link]

[6] Fuyuan Xu et al., "Water Balance Analysis and Wastewater Recycling Investigation in Electrolytic Manganese Industry of China — A Case Study," *Hydrometallurgy*, vol. 149, pp. 12-22, 2014. [CrossRef] [Google Scholar] [Publisher Link]

[7] Fan Wang et al., "Application of Electrolytic Manganese Residues in Cement Products through Pozzolanic Activity Motivation and Calcination," *Journal of Cleaner Production*, vol. 338, 2022. [CrossRef] [Google Scholar] [Publisher Link]

[8] Ali Allahverdi, and Salim Ahmadnezhad, "Mechanical Activation of Silicomanganese Slag and its Influence on the Properties of Portland Slag Cement," *Powder Technology*, vol. 251, pp. 41-51, 2014. [CrossRef] [Google Scholar] [Publisher Link]

[9] Kefei Li et al., "Effect of Self-Desiccation on the Pore Structure of Paste and Mortar Incorporating 70% GGBS," *Construction and Building Materials*, vol. 51, pp. 329-337, 2014. [CrossRef] [Google Scholar] [Publisher Link]

[10] Mohammad Bolhassani, and Mohammadreza Samani, "Effect of Type, Size, and Dosage of Nanosilica and Microsilica on Properties of Cement Paste and Mortar," *Materials Journal*, vol. 112, no. 2, pp. 259-266, 2015. [CrossRef] [Google Scholar] [Publisher Link]

[11] Quentin Colombet, Florian Brandner, and Alain Darte, "Studying Optimal Spilling in the Light of SSA," *ACM Transactions on Architecture and Code Optimization (TACO)*, vol. 11, no. 4, pp. 1-26, 2015. [CrossRef] [Google Scholar] [Publisher Link]

[12] Jue Wang, and Xiang Li, "A Combined Neural Network Model for Commodity Price Forecasting with SSA," *Soft Computing*, vol. 22, pp. 5323-5333, 2018. [CrossRef] [Google Scholar] [Publisher Link]

[13] Moisés Frias et al., "Recycling of Silicomanganese Slag as Pozzolanic Material in Portland Cements: Basic and Engineering Properties," *Cement and Concrete Research*, vol. 36, no. 3, pp. 487-491, 2006. [CrossRef] [Google Scholar] [Publisher Link]

[14] Benjun Wang et al., "Lead Leaching Mechanism and Kinetics in Electrolytic Manganese Anode Slime," *Hydrometallurgy*, vol. 183, pp. 98-105, 2019. [CrossRef] [Google Scholar] [Publisher Link]

[15] Changbo Zhou, Jiwei Wang, and Nanfang Wang, "Treating Electrolytic Manganese Residue with Alkaline Additives for Stabilizing Manganese and Removing Ammonia," *Korean Journal of Chemical Engineering*, vol. 30, pp. 2037-2042, 2013. [CrossRef] [Google Scholar] [Publisher Link]

[16] S.K. Nath, and Sanjay Kumar, "Evaluation of the Suitability of Ground Granulated Silico-Manganese Slag in Portland Slag Cement," *Construction and Building Materials*, vol. 125, pp. 127-134, 2016. [CrossRef] [Google Scholar] [Publisher Link]

[17] Bassam A. Tayeh et al., "Durability and Mechanical Properties of Cement Concrete Comprising Pozzolanic Materials with Alkali-Activated Binder: A Comprehensive Review," *Case Studies in Construction Materials*, vol. 17, pp. 1-17, 2022. [CrossRef] [Google Scholar] [Publisher Link]

[18] Caijun Shi et al., "The Hydration and Microstructure of Ultra High-Strength Concrete with Cement–Silica Fume–Slag Binder," *Cement and Concrete Composites*, vol. 61, pp. 44-52, 2015. [CrossRef] [Google Scholar] [Publisher Link]

[19] Kaffayatullah Khan, and Muhammad Nasir Amin, "Influence of Fineness of Volcanic Ash and its Blends with Quarry Dust and Slag on Compressive Strength of Mortar under Different Curing Temperatures," *Construction and Building Materials*, vol. 154, pp. 514-528, 2017. [CrossRef] [Google Scholar] [Publisher Link]

[20] Jae-Won Her, and Nam-Gi Lim, "Physical and Chemical Properties of Nano-Slag Mixed Mortar," *Journal of the Korea Institute of Building Construction*, vol. 10, no. 6, pp. 145-154, 2010. [CrossRef] [Google Scholar] [Publisher Link]

[21] Jinpeng Dai et al., "The Effect of Fineness on the Hydration Activity Index of Ground Granulated Blast Furnace Slag," *Materials*, vol. 12, no. 18, pp. 1-15, 2019. [CrossRef] [Google Scholar] [Publisher Link]

[22] Ruben Snellings, Prannoy Suraneni, and Jørgen Skibsted, "Future and Emerging Supplementary Cementitious Materials," *Cement and Concrete Research*, vol. 171, 2023. [CrossRef] [Google Scholar] [Publisher Link]

[23] Jialei Wang et al., "The Role and Mechanism of Rice Husk Ash Particle Characteristics in Cement Hydration Process," *Materials*, vol. 17, no. 22, pp. 1-21, 2024. [CrossRef] [Google Scholar] [Publisher Link]

[24] Chee Khoon Ng et al., "The Properties of Normal Concrete with Ground Manganese Slag as Binder Replacement," *Journal of Advanced Research in Applied Mechanics*, vol. 116, no. 1, pp. 62-74, 2024. [CrossRef] [Google Scholar] [Publisher Link]

[25] Libo Zhou et al., "Study on the Mechanical Properties and Hydration Behavior of Steel Slag–Red Mud–Electrolytic Manganese Residue Based Composite Mortar," *Applied Sciences*, vol. 13, no. 10, pp. 1-14, 2023. [CrossRef] [Google Scholar] [Publisher Link]

[26] H. Alperen Bulut, and Remzi Şahin, "Radiological Characteristics of Self-Compacting Concretes Incorporating Fly Ash, Silica Fume, and Slag," *Journal of Building Engineering*, vol. 58, 2022. [CrossRef] [Google Scholar] [Publisher Link]

[27] Jingjing He et al., "Study on the Effect of Silica–Manganese Slag Mixing on the Deterioration Resistance of Concrete under the Action of Salt Freezing," *Buildings*, vol. 14, no. 9, pp. 1-20, 2024. [CrossRef] [Google Scholar] [Publisher Link]

[28] Junchao Yang et al., "The Properties of High-Performance Concrete with Manganese Slag under Salt Action," *Materials*, vol. 17, no. 7, pp. 1-20, 2024. [CrossRef] [Google Scholar] [Publisher Link]

[29] Farzaneh Elyasigorji et al., "Comprehensive Review of Direct and Indirect Pozzolanic Reactivity Testing Methods," *Building*s, vol. 13, no. 11, pp. 1-26, 2023. [CrossRef] [Google Scholar] [Publisher Link]

[30] Rong-jin Liu et al., "Durability of Concrete Made with Manganese Slag as Supplementary Cementitious Materials," *Journal of Shanghai Jiaotong University (Science)*, vol. 17, pp. 345-349, 2012. [CrossRef] [Google Scholar] [Publisher Link]

[31] Mike Otieno, Hans Beushausen, and Mark Alexander, "Effect of Chemical Composition of Slag on Chloride Penetration Resistance of Concrete," *Cement and Concrete Composites*, vol. 46, pp. 56-64, 2014. [CrossRef] [Google Scholar] [Publisher Link]

[32] Yingtang Xu et al., "Investigation on Sulfate Activation of Electrolytic Manganese Residue on Early Activity of Blast Furnace Slag in Cement-Based Cementitious Material," *Construction and Building Materials*, vol. 229, 2019. [CrossRef] [Google Scholar] [Publisher Link]

[33] Demet Demir Şahin, and Hasan Eker, "Effects of Ultrafine Fly Ash against Sulphate Reaction in Concrete Structures," *Materials*, vol. 17, no. 6, pp. 1-20, 2024. [CrossRef] [Google Scholar] [Publisher Link]

[34] Kevin D. Copeland et al., "Ultra Fine Fly Ash for High Performance Concrete," *Construction and Materials Issues 2001*, pp. 166-175, 2001. [CrossRef] [Google Scholar] [Publisher Link]

[35] Yoram Wind, and Thomas L. Saaty, "Marketing Applications of the Analytic Hierarchy Process," *Management Science*, vol. 26, no. 7, pp. 641-658, 1980. [CrossRef] [Google Scholar] [Publisher Link]

[36] Yuyan Shen, and Kaicheng Liao, "An Application of Analytic Hierarchy Process and Entropy Weight Method in Food Cold Chain Risk Evaluation Model," *Frontiers in Psychology*, vol. 13, pp. 1-13, 2022. [CrossRef] [Google Scholar] [Publisher Link]
[37] Huawang Shi et al., "Durability Evaluation of Iron Tailings Concrete under Freeze-Thaw Cycles and Sulfate Erosion Based on Entropy Weighting Method," *Construction and Building Materials*, vol. 443, 2024. [CrossRef] [Google Scholar] [Publisher Link]
[38] Jinru Wu, Xiaoling Chen, and Jianzhong Lu, "Assessment of Long and Short-Term Flood Risk Using the Multi-Criteria Analysis Model with the AHP-Entropy Method in Poyang Lake Basin," *International Journal of Disaster Risk Reduction*, vol. 75, 2022. [CrossRef] [Google Scholar] [Publisher Link]
[39] Le Zhang, Xueyan Li, and Yanlong Guo, "Research on the Influencing Factors of Spatial Vitality of Night Parks Based on AHP–Entropy Weights," *Sustainability*, vol. 16, no. 12, pp. 1-20, 2024. [CrossRef] [Google Scholar] [Publisher Link]
[40] Gang Han et al., "Evaluation of the Ventilation Mode in an ISO Class 6 Electronic Cleanroom by the AHP-Entropy Weight Method," *Energy*, vol. 284, 2023. [CrossRef] [Google Scholar] [Publisher Link]
[41] Juan-Juan Ren et al., "Evaluation of Slab Track Quality Indices Based on Entropy Weight-Fuzzy Analytic Hierarchy Process," *Engineering Failure Analysis*, vol. 149, 2023. [CrossRef] [Google Scholar] [Publisher Link]
[42] Peter Fernandes Wanke et al., "An Original Information Entropy-Based Quantitative Evaluation Model for Low-Carbon Operations in an Emerging Market," *International Journal of Production Economics*, vol. 234, 2021. [CrossRef] [Google Scholar] [Publisher Link]
[43] BS EN 12350-2:2019 - TC, Testing Fresh Concrete - Slump Test, Bsi.knowledge, 2019. [Online]. Available: https://knowledge.bsigroup.com/products/testing-fresh-concrete-slump-test-2
[44] BS EN 12390-3:2019 - TC, Testing Hardened Concrete - Compressive Strength of Test Specimens, Bsi.knowledge, 2019. [Online]. Available: https://knowledge.bsigroup.com/products/testing-hardened-concrete-compressive-strength-of-test-specimens-1
[45] BS EN 12390-5:2019 - TC, Testing Hardened Concrete - Flexural Strength of Test Specimens, Bsi.knowledge, 2019. [Online]. Available: https://knowledge.bsigroup.com/products/testing-hardened-concrete-flexural-strength-of-test-specimens-1
[46] ASTM C1202-17, Standard Test Method for Electrical Indication of Concrete's Ability to Resist Chloride Ion Penetration, ASTM, 2017. [Online]. Available: https://store.astm.org/c1202-17.html
[47] ASTM C1012/C1012M-15, Standard Test Method for Length Change of Hydraulic-Cement Mortars Exposed to a Sulfate Solution, ASTM, 2018. [Online]. Available: https://store.astm.org/c1012_c1012m-15.html
[48] ASTM C157/C157M-17, Standard Test Method for Length Change of Hardened Hydraulic-Cement Mortar and Concrete, ASTM, 2017. [Online]. Available: https://store.astm.org/c0157_c0157m-17.html
[49] PD CEN/TS 12390-9:2016 - TC, Testing Hardened Concrete - Freeze-Thaw Resistance with De-Icing Salts. Scaling, Bsi.knowledge, 2016. [Online]. Available: https://knowledge.bsigroup.com/products/testing-hardened-concrete-freeze-thaw-resistance-with-de-icing-salts-scaling
[50] Amos Darko et al., "Review of Application of Analytic Hierarchy Process (AHP) in Construction," *International Journal of Construction Management*, vol. 19, no. 5, pp. 436-452, 2019. [CrossRef] [Google Scholar] [Publisher Link]